Activation of ethylene and ammonia at iridium: C–H *versus* N–H oxidative addition†

Marcel Ahijado Salomon, Ann-Katrin Jungton and Thomas Braun*

Received 30th March 2009, Accepted 12th June 2009
First published as an Advance Article on the web 27th July 2009
DOI: 10.1039/b906189d

The ammine complexes *cis-trans*-[Ir(4-C_5NF_4)(H)$_2$(NH_3)(P*i*Pr$_3$)$_2$] (**3**) and *cis*-[Ir(4-C_5NF_4)(H){(*E*)-(MeO_2C)*C*=CH(CO_2Me)}(NH_3)$_2$(P*i*Pr$_3$)] (**5**) are generated on reaction of *cis-trans*-[Ir(4-C_5NF_4)(H)$_2$-(P*i*Pr$_3$)$_2$] (**1**) or of the vinyl compound *trans*-[Ir(4-C_5NF_4)(H){(*E*)-(MeO_2C)*C*=CH(CO_2Me)}-(P*i*Pr$_3$)$_2$] (**4**) with NH_3, respectively. Photolysis of **5** gives complex [Ir(4-C_5NF_4)(H){κ^2-(*C,O*)-(*Z*)-(MeO_2C)*C*=CH(C*O*OMe)}(NH_3)(P*i*Pr$_3$)] (**6**). Treatment of the ethylene compound *trans*-[Ir(4-C_5NF_4)-(C_2H_4)(P*i*Pr$_3$)$_2$] (**2**) with ammonia yields C–H activation products such as the hydrido vinyl species *trans*-[Ir(4-C_5NF_4)(H)(C_2H_3)(NH_3)(P*i*Pr$_3$)$_2$] (**7**) and the cyclometallation products [Ir(4-C_5NF_4)(H)-(NH_3){κ^2-(*P,C*)-*C*H_2CH(CH_3)P*i*Pr$_2$}(P*i*Pr$_3$)] (**8a**, **8b**). A subsequent reaction leads to the generation of the binuclear oxidative addition product of ammonia [Ir(4-C_5NF_4)(H)(μ-NH_2)(NH_3)(P*i*Pr$_3$)]$_2$ (**9**).

Introduction

An attractive route to use ammonia as a feedstock for the synthesis of amines consists of its functionalization in homogeneous catalytic reactions.[1,2] Catalytic couplings of aryl halides with ammonia in the presence of a base and a palladium or copper catalyst have been realized.[3] Homogeneous catalytic reductive aminations of benzaldehydes with ammonia have also been accomplished in the presence of hydrogen to give primary amines.[4] A selective synthesis of primary amines directly from alcohols and ammonia has been reported very recently by Gunanathan and Milstein. The transformations are catalyzed by a ruthenium pincer complex.[5] They presumably proceed *via* an intermediate aldehyde and imine and produce water as by-product. A recent report on the hydroamination of alkynes and allenes with ammonia can be considered as another breakthrough.[6] The process is catalyzed by a cationic gold carbene complex and yields imines, enamines or allyl amines. Mechanistically, the insertion of the organic substrate into the metal–nitrogen bond of an amido ligand has been proposed as a possible key-step.[6,7] A related suggestion involves coordination of the amine to the gold centre prior to the C–N bond formation.[8]

The oxidative addition of ammonia can be regarded as a model reaction for the development of new catalytic reaction cycles which involve an N–H bond cleavage in NH_3 by the insertion of a transition metal as a key-step.[2] Usually ammonia generates in the coordination sphere of a transition metal simple "Werner-like" Lewis acid–base adducts, although there is some precedent for the activation of ammonia by transition-metal complexes *via* various reaction pathways.[9,10] So far, very little has been reported on an oxidative addition reaction.[11–15] A significant discovery involves the oxidative addition of ammonia at an iridium(I) complex which exhibits a tridentate pincer ligand.[15]

Humboldt-Universität zu Berlin, Institut für Chemie, Brook-Taylor-Str., 2, 12489, Berlin, Germany. E-mail: thomas.braun@chemie.hu-berlin.de

† CCDC reference numbers 725696–725700. For crystallographic data in CIF or other electronic format see DOI: 10.1039/b906189d

We demonstrated recently that complex *cis-trans*-[Ir(4-C_5NF_4)(H)$_2$(P*i*Pr$_3$)$_2$] (**1**) reacts with ethylene to yield the tetrafluoropyridyl complex *trans*-[Ir(4-C_5NF_4)(C_2H_4)(P*i*Pr$_3$)$_2$] (**2**).[16] The iridium–carbon bond in **1** is surprisingly stable and no reductive elimination product has been observed.

In this paper we report on the reactivity of ammonia towards the iridium(I) and iridium(III) tetrafluoropyridyl complexes such as **1** and **2**. Complexes which bear a tetrafluoropyridyl ligand often exhibit an unusual stability.[17] This led us to investigate the properties of iridium(I) and iridium(III) derivatives, towards C–H and N–H activation reactions. We envisaged the generation of an oxidative addition product of ammonia bearing a C_4NF_4 ligand at iridium. In contrast to reactions at the {IrCl(P*i*Pr$_3$)$_2$} moiety the generation of cationic compounds is at {Ir(4-C_5NF_4)(P*i*Pr$_3$)$_2$} not feasible.[2,12]

Results

Formation of ammine complexes

A reaction of *cis-trans*-[Ir(4-C_5NF_4)(H)$_2$(P*i*Pr$_3$)$_2$] (**1**) with ammonia gave solely the "Werner-type" ammine complex *cis-trans*-[Ir(4-C_5NF_4)(H)$_2$(NH_3)(P*i*Pr$_3$)$_2$] (**3**) (Scheme 1). A singlet in the ^{31}P{^{1}H} NMR spectrum of **3** at δ 30.6 confirms the *trans* orientation of the phosphine ligands. The ^{19}F NMR spectrum shows four resonances which suggests a restricted rotation about the tetrafluoropyridyl ligand.[16,17] The presence of the two hydrido ligands is revealed in the ^{1}H NMR spectrum by two signals at δ −14.72 and δ −24.02. The coordinated ammine leads to a resonance at δ(^{15}N) −88 in the ^{1}H–^{15}N NMR HBMC spectrum of the isotopomer *trans*-[Ir(4-C_5NF_4)(H)$_2$($^{15}NH_3$)(P*i*Pr$_3$)$_2$] (**3′**). A ^{1}H NMR EXSY (400 MHz) spectrum of **3** exhibits cross-peaks with a positive sign with respect to the diagonal peaks confirming exchange of metal bound hydrogens. There is no indication for an exchange of ammine protons and metal bound hydrogens.[10] Moreover, we did not find any reductive elimination of 2,3,5,6-tetrafluoropyridine.[18]

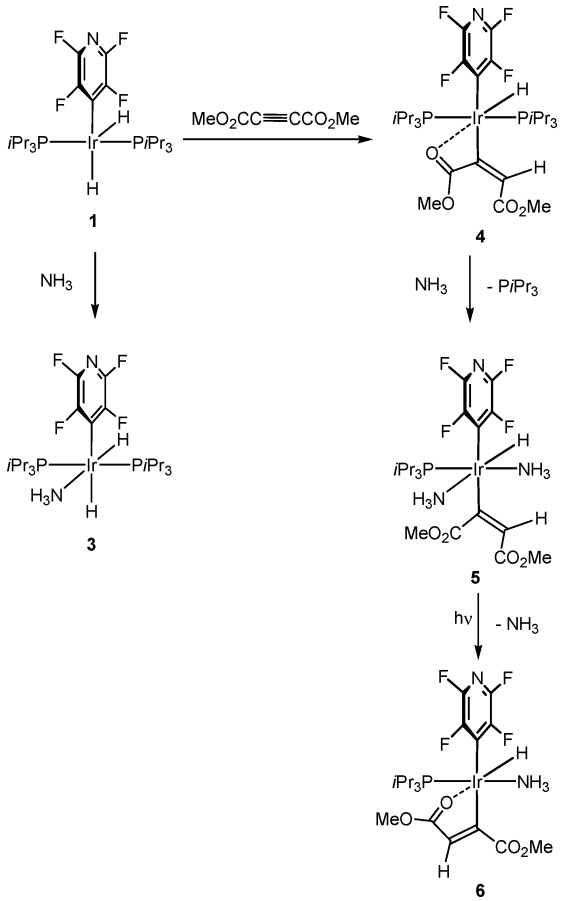

Scheme 1 Formation of vinyl ammine complexes.

The molecular structure of **3** was confirmed by X-ray diffraction analysis at 100 K (Fig. 1). Selected bond lengths and angles are summarised in Table 1. The structure reveals an octahedral configuration with the expected *trans* disposition of the phosphine ligands. The hydrides at iridium have been located and found to be in a *cis* position. The separation between H(1A) and H(1B) is 2.100 Å. The iridium-carbon distance is 2.144(2) Å. For comparison, the Ir–C separation of 2.144(4) Å in the complex *cis-trans*-[Ir(4-C_5NF_4)$(H)_2(P{i}Pr_3)_2$] (**1**) is similar.[16]

Table 1 Selected bond lengths (Å) and angles (°) in *cis-trans*-[Ir(4-C_5NF_4)$(H)_2(P{i}Pr_3)_2(NH_3)$] (**3**) with estimated standard deviations in parentheses

Ir(1)–P(1)	2.3098(8)	C(19)–C(20)	1.402(3)
Ir(1)–P(2)	2.3111(8)	C(20)–C(21)	1.374(4)
Ir(1)–N(1)	2.251(2)	C(22)–C(23)	1.380(4)
Ir(1)–C(19)	2.144(2)	C(19)–C(23)	1.396(3)
Ir(1)–H(1A)	1.43(2)	C(20)–F(1)	1.361(3)
Ir(1)–H(1B)	1.38(2)	C(21)–F(2)	1.349(3)
N(2)–C(22)	1.312(3)	C(22)–F(3)	1.350(3)
N(2)–C(21)	1.310(3)	C(23)–F(4)	1.355(3)
P(1)–Ir(1)–P(2)	164.82(2)	Ir(1)–C(19)–C(20)	126.83(18)
N(1)–Ir(1)–P(1)	90.38(6)	C(23)–C(19)–C(20)	109.1(2)
N(1)–Ir(1)–P(2)	98.92(6)	C(21)–C(20)–C(19)	123.8(2)
C(19)–Ir(1)–N(1)	96.44(9)	N(2)–C(21)–C(20)	124.9(2)
C(19)–Ir(1)–P(1)	95.98(7)	C(21)–N(2)–C(22)	113.8(2)
C(19)–Ir(1)–P(2)	94.87(7)	N(2)–C(22)–C(23)	124.8(2)
Ir(1)–C(19)–C(23)	124.06(18)		

Furthermore, we synthesised an iridium(III) hydrido vinyl complex, which features in contrast to the dihydride **1** an additional iridium-carbon bond. Treatment of complex **1** with acetylene dicarboxylate $MeO_2CC{\equiv}CCO_2Me$ resulted in a colour change from yellow to red within two hours to give *trans*-[Ir(4-C_5NF_4)(H){(*E*)-$(MeO_2C)C{=}CH(CO_2Me)$}$(P{i}Pr_3)_2$] (**4**) (Scheme 1). It has been reported that the chloro complex [Ir(Cl)(H){(*E*)-$(MeO_2C)C{=}CH(CO_2Me)$}$(P{i}Pr_3)_2$] can be prepared in a similar manner.[19] Compound **4** exhibits a singlet at δ 17.4 in the $^{31}P\{^1H\}$ NMR spectrum which can be assigned to the *trans* phosphines. The presence of four signals in the ^{19}F NMR spectrum again indicates a hindered rotation of the tetrafluoropyridyl ligand about the Ir–C bond. The IR spectrum of **4** exhibits an absorption band at 2338 cm^{-1} which can be assigned to the IrH moiety.[19]

The molecular structure of **4** was also confirmed by X-ray diffraction analysis at 170 K (Fig. 2, Table 2). The structure reveals a square pyramidal configuration with the expected *trans* disposition of the phosphine ligands. There is a significant

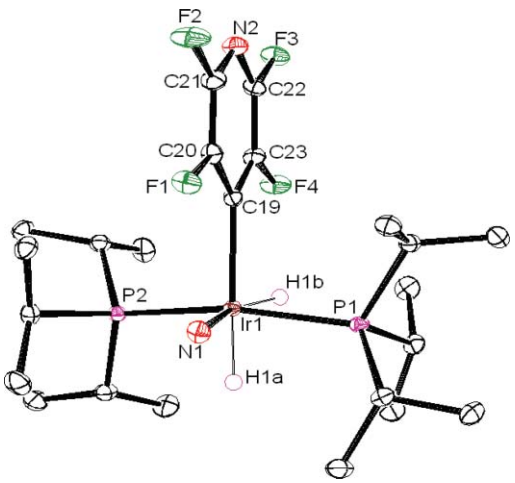

Fig. 1 An ORTEP diagram of **3**; Ellipsoids are drawn at the 50% probability level; Hydrogen atoms have been omitted for clarity, except for metal bound hydrogens.

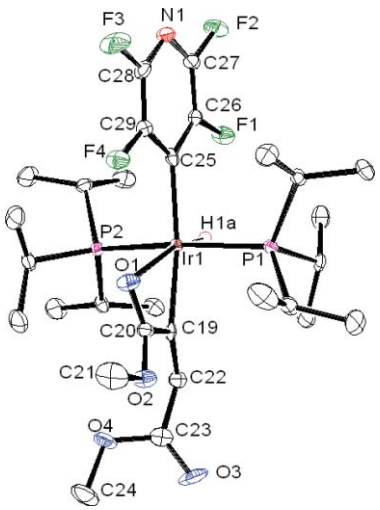

Fig. 2 An ORTEP diagram of **4**; Ellipsoids are drawn at the 50% probability level; hydrogen atoms have been omitted for clarity, except for metal bound hydrogen.

Table 2 Selected bond lengths (Å) and angles (°) in *trans*-[Ir(4-C_5NF_4)(H){(*E*)-(MeO_2C)*C*=CH(CO_2Me)}($PiPr_3$)$_2$] (**4**) with estimated standard deviations in parentheses

Ir(1)–P(1)	2.3651(9)	C(22)–C(23)	1.475(4)
Ir(1)–P(2)	2.3583(9)	N(1)–C(27)	1.316(4)
Ir(1)–H(1a)	1.54(3)	N(1)–C(28)	1.311(4)
Ir(1)–C(19)	2.084(3)	C(25)–C(26)	1.412(5)
Ir(1)–C(25)	2.093(3)	C(26)–C(27)	1.357(4)
Ir(1)–O(1)	2.446(2)	C(28)–C(29)	1.360(4)
C(20)–O(1)	1.230(4)	C(25)–C(29)	1.402(4)
C(20)–O(2)	1.325(4)	C(26)–F(1)	1.369(4)
C(23)–O(3)	1.206(4)	C(27)–F(2)	1.356(3)
C(23)–O(4)	1.351(4)	C(28)–F(3)	1.357(3)
C(19)–C(22)	1.339(4)	C(29)–F(4)	1.366(3)
C(19)–Ir(1)–C(25)	166.57(12)	N(1)–C(27)–C(26)	125.3(3)
P(2)–Ir(1)–P(1)	166.55(3)	N(1)–C(28)–C(29)	125.5(3)
P(2)–Ir(1)–O(1)	94.28(6)	C(25)–C(26)–C(27)	123.6(3)
C(19)–Ir(1)–P(1)	89.71(8)	C(25)–C(29)–C(28)	123.7(3)
C(19)–Ir(1)–P(2)	88.50(8)	C(26)–C(25)–C(29)	108.7(3)
P(1)–Ir(1)–O(1)	96.51(6)	Ir(1)–O(1)–C(20)	86.07(18)
C(19)–Ir(1)–O(1)	61.11(9)	Ir(1)–C(19)–C(22)	143.9(2)
C(25)–Ir(1)–P(1)	92.50(9)	C(19)–C(22)–C(23)	127.2(3)
C(25)–Ir(1)–P(2)	92.32(9)	O(1)–C(20)–C(19)	116.9(3)
C(25)–Ir(1)–O(1)	105.47(11)	O(1)–C(20)–O(2)	122.8(3)
Ir(1)–C(25)–C(29)	121.4(2)	O(3)–C(23)–C(22)	124.6(3)
Ir(1)–C(25)–C(26)	129.8(3)	O(3)–C(23)–O(4)	123.4(4)
C(28)–N(1)–C(27)	113.2(3)		

Table 3 Selected bond lengths (Å) and angles (°) in [Ir(4-C_5NF_4)(H){(*E*)-(MeO_2C)*C*=CH(CO_2Me)}(NH_3)$_2$($PiPr_3$)] (**5**) with estimated standard deviations in parentheses

Ir(1)–N(1)	2.172(5)	N(3)–C(12)	1.295(10)
Ir(1)–N(2)	2.235(5)	N(3)–C(13)	1.318(9)
Ir(1)–P(1)	2.2634(16)	C(10)–C(11)	1.371(9)
Ir(1)–C(10)	2.085(6)	C(10)–C(14)	1.403(9)
Ir(1)–C(15)	2.113(6)	C(11)–C(12)	1.381(9)
C(16)–O(1)	1.204(8)	C(13)–C(14)	1.373(9)
C(16)–O(2)	1.353(7)	C(11)–F(1)	1.368(8)
C(19)–O(3)	1.219(9)	C(12)–F(2)	1.348(8)
C(19)–O(4)	1.342(9)	C(13)–F(3)	1.345(8)
C(15)–C(18)	1.341(9)	C(14)–F(4)	1.371(8)
C(18)–C(19)	1.472(9)		
N(1)–Ir(1)–P(1)	172.07(16)	C(12)–N(3)–C(13)	114.6(6)
N(2)–Ir(1)–P(1)	104.75(15)	N(3)–C(12)–C(11)	124.6(7)
N(1)–Ir(1)–N(2)	83.1(2)	N(3)–C(13)–C(14)	124.0(7)
C(10)–Ir(1)–N(1)	81.7(2)	C(10)–C(11)–C(12)	123.4(2)
C(15)–Ir(1)–N(1)	84.4(2)	C(13)–C(14)–C(10)	122.8(7)
C(10)–Ir(1)–N(2)	92.6(2)	Ir(1)–C(15)–C(18)	121.9(5)
C(15)–Ir(1)–N(2)	90.1(2)	Ir(1)–C(15)–C(16)	120.5(4)
C(10)–Ir(1)–P(1)	96.64(10)	C(15)–C(18)–C(19)	125.4(6)
C(15)–Ir(1)–P(1)	96.59(17)	O(1)–C(16)–O(2)	123.0(6)
C(10)–Ir(1)–C(15)	165.4(2)	O(1)–C(16)–C(15)	126.5(6)
Ir(1)–C(10)–C(11)	122.8(5)	O(3)–C(19)–O(4)	123.4(7)
Ir(1)–C(10)–C(14)	126.0(5)	O(3)–C(19)–C(18)	125.9(7)

additional contact of one of the ester groups to iridium with an O(1)–Ir(1) distance of 2.447(2) Å, which completes an octahedral coordination sphere at the metal centre. This is reflected in the C=O separations which are 1.230(4) Å for the ester group bound to iridium and 1.206(4) Å for the distal ester group. The *cis* arrangement of the ester moieties at the carbon-carbon double bond results in the formation of a four-membered ring. A comparable four-membered chelate has been found in *trans*-[Ir($C_3N_2H_4$)(H)(MeO_2CC=CH_2)(PPh_3)$_2$]BF_4 with an iridium oxygen distance of 2.28(1) Å.[20] The dihedral angle between the plane defined by the pyridyl ring and the coordination plane of the metal defined by Ir1, C19, C25, P1 and P2 is 86.2°. The iridium-carbon distance to the pyridyl ring is 2.095(3) Å. For comparison, the Ir–C separation of 2.144(4) in **1** is in a similar range.[12] The metal-carbon bond length to the vinyl group is 2.084(3) Å.

The hydride compound **4** reacted with NH_3 to afford free $PiPr_3$ and the monophosphine complex *cis*-[Ir(4-C_5NF_4)(H){(*E*)-(MeO_2C)*C*=CH(CO_2Me)}(NH_3)$_2$($PiPr_3$)] (**5**) (Scheme 1). The $^{31}P\{^1H\}$ NMR spectrum of **5** displays a singlet at δ 13.9 for the phosphine. The ^{31}P NMR spectrum of the isotopomer *cis*-[Ir(4-C_5NF_4)(H){(*E*)-(MeO_2C)*C*=CH(CO_2Me)}($^{15}NH_3$)$_2$($PiPr_3$)] (**5′**) exhibits one additional coupling to nitrogen of 46.7 Hz, presumably to the ammine ligand in the *trans* position to the phosphorus. The ^{19}F NMR spectrum of **5** depicts four resonances for the tetrafluoropyridyl ligand. The signal for the hydrido ligand appears at δ −28.09 in the ^1H NMR spectrum. The phosphorus–hydrogen coupling of 13.8 Hz suggests a *cis* arrangement of metal bound phosphorus and hydrogen. The molecular structure of the octahedral complex **5** was also determined by X-ray diffraction at 100 K (Fig. 3, Table 3). Neither the iridium-carbon distance to the C_5NF_4 unit of 2.085(6) Å nor the iridium-carbon distance to the vinyl group of 2.113(6) Å show a significant difference to the Ir–C distances found in **4**.

Prolonged heating of a benzene of **5** solution at 50 °C did not lead to any reduction elimination reaction. However photolysis

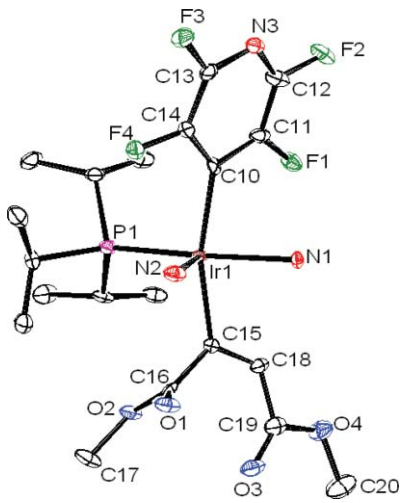

Fig. 3 An ORTEP diagram of **5**; ellipsoids are drawn at the 50% probability level; hydrogen atoms and a benzene solvent molecule have been omitted for clarity.

led to a *cis-trans* isomerisation at the C=C double bond with a concomitant dissociation of one ammonia molecule and complex [Ir(4-C_5NF_4)(H){κ^2-(*C,O*)-(*Z*)-(MeO_2C)*C*=CH(C*O*OMe)}(NH_3)($PiPr_3$)] (**6**) was generated (Scheme 1). A comparable *cis-trans* isomerisation has been observed at [Ir(Cl)(H){(*E*)-(MeO_2C)*C*=CH(CO_2Me)}($PiPr_3$)$_2$] to yield [Ir(Cl)(H){κ^2-(*C,O*)-(*Z*)-(MeO_2C)*C*=CH(C*O*OMe)}($PiPr_3$)$_2$].[19] Complex **6** resembles the structure of **4**, but one phosphine has been replaced by an ammine ligand. In addition, the ester groups are now orientated in a *trans* position at the vinyl double bond, which leads to the formation of a five-membered ring. The ^1H NMR spectrum depicts a signal at −28.36 with a doublet coupling to the phosphorus nucleus of 21.9 Hz which is characteristic for a *cis* orientation of the phosphine ligand and the hydride. The IR spectrum of **6** shows

Table 4 Selected bond lengths (Å) and angles (°) in [Ir(4-C_5NF_4)(H){κ²-(*C,O*)-(*Z*)-(MeO_2C)*C*=CH(*C*O*O*Me)}(NH_3)(P*i*Pr_3)] (**6**) with estimated standard deviations in parentheses

Ir(1)–N(1)	2.1601(18)	C(17)–C(19)	1.480(3)
Ir(1)–O(1)	2.2700(16)	C(10)–C(14)	1.396(3)
Ir(1)–P(1)	2.2608(6)	C(10)–C(11)	1.386(3)
Ir(1)–H(1d)	1.44(3)	C(13)–C(14)	1.378(3)
Ir(1)–C(10)	2.102(2)	C(11)–C(12)	1.373(3)
Ir(1)–C(17)	2.049(2)	N(2)–C(12)	1.316(3)
C(15)–O(1)	1.237(3)	N(2)–C(13)	1.307(3)
C(15)–O(2)	1.328(3)	C(11)–F(1)	1.363(3)
C(19)–O(3)	1.211(3)	C(12)–F(2)	1.350(3)
C(19)–O(4)	1.341(3)	C(13)–F(3)	1.349(3)
C(15)–C(16)	1.452(3)	C(14)–F(4)	1.351(3)
C(16)–C(17)	1.350(3)		
N(1)–Ir(1)–P(1)	178.20(5)	C(13)–N(2)–C(12)	114.2(2)
C(17)–Ir(1)–C(10)	168.74(9)	C(12)–C(11)–C(10)	122.8(2)
P(1)–Ir(1)–O(1)	100.16(4)	N(2)–C(12)–C(11)	124.8(2)
N(1)–Ir(1)–O(1)	81.60(7)	N(2)–C(13)–C(14)	124.7(2)
C(17)–Ir(1)–P(1)	95.07(6)	C(13)–C(14)–C(10)	122.6(2)
C(17)–Ir(1)–N(1)	84.95(8)	Ir(1)–C(17)–C(16)	116.93(16)
C(17)–Ir(1)–O(1)	76.45(8)	Ir(1)–C(17)–C(19)	124.00(17)
C(17)–Ir(1)–H(1d)	100.9(11)	Ir(1)–O(1)–C(15)	109.47(14)
C(10)–Ir(1)–P(1)	95.90(6)	O(1)–C(15)–C(16)	122.4(2)
C(10)–Ir(1)–N(1)	84.16(8)	O(1)–C(15)–O(2)	121.6(2)
C(10)–Ir(1)–O(1)	99.08(7)	O(3)–C(19)–O(4)	122.1(2)
Ir(1)–C(10)–C(11)	124.23(16)	C(15)–C(16)–C(17)	114.4(2)
Ir(1)–C(10)–C(14)	124.22(16)	C(16)–C(17)–C(19)	117.6(2)

an absorption band at 2280 cm^{-1} which can be assigned to the IrH moiety.[16,19]

The configuration of **6** at the metal centre was revealed by X-ray diffraction analysis at 100 K (Fig. 4, Table 4). The iridium–carbon distances to the C_5NF_4 unit of 2.102(2) Å and to the vinyl group of 2.049(2) Å are comparable to the separations found in **4** and **5** and are in the expected range. The *trans* arrangement of the ester moieties at the carbon-carbon double bond results, in contrast to the situation in **4**, in the formation of a five-membered ring. The C=O separations are 1.237(3) Å for the ester group bound to iridium and 1.211(3) Å for the distal ester group. These values are consistent with the literature data.[21]

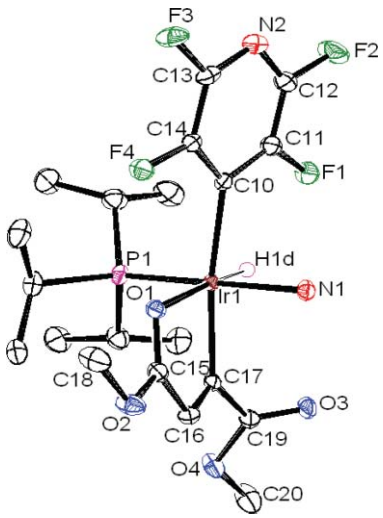

Fig. 4 An ORTEP diagram of **6**; ellipsoids are drawn at the 50% probability level; hydrogen atoms and a benzene solvent molecule have been omitted for clarity, except for metal bound hydrogen.

C–H *via* N–H bond activation

In contrast to the reactions at Ir(III), in which only coordination of ammonia has been achieved, the presence of ammonia at Ir(I) leads either to C–H activation or to an oxidative addition of a N–H bond. Thus, treatment of the iridium(I) ethylene complex *trans*-[Ir(4-C_5NF_4)(C_2H_4)(P*i*Pr_3)$_2$] (**2**) with NH_3 furnishes initially the C–H activation product *trans*-[Ir(4-C_5NF_4)(H)(C_2H_3)(NH_3)(P*i*Pr_3)$_2$] (**7**) (Scheme 2). Complex **7** could not be isolated in the solid state, because it reacts further to give the two isomeric cyclometallation products [Ir(4-C_5NF_4)(H)(NH_3){κ²-(*P,C*)-*C*H_2CH(CH_3)P*i*Pr_2}(P*i*Pr_3)] (**8a**, **8b**) as well as free ethylene. The latter two were detected in the NMR spectra.

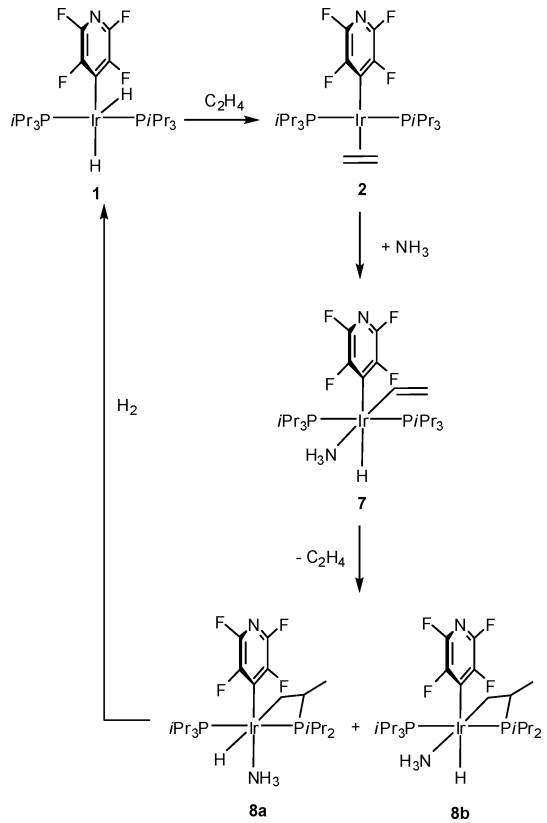

Scheme 2 C–H activation at ammine complexes.

The $^{31}P\{^1H\}$ NMR spectrum of **7** displays a singlet at δ 1.8 for the phosphines in the mutually *trans* position. The ^{19}F NMR spectrum depicts four resonances for the tetrafluoropyridyl ligand. The ^1H NMR spectrum shows a triplet of doublets at δ –21.88 for the hydride at the iridium center. On ^{31}P decoupling the signal simplifies to a doublet with a hydrogen-fluorine coupling of 9.3 Hz. Note that the latter is not indicative for a *trans* arrangement of the hydride and fluoropyridyl moiety.[16] The presence of the vinyl ligand is revealed by resonances at δ 8.36, δ 6.03 and δ 5.02. A ^1H–^{13}C HMQC NMR spectrum exhibits resonances at δ 143.6 and δ 116.6 in the ^{13}C domain for the α- and β- carbon atom in the vinyl group, respectively. The presence of the ammine ligand is revealed in the ^1H–^{15}N NMR spectrum of the isotopologue *trans*-[Ir(4-C_5NF_4)(H)(C_2H_3)($^{15}NH_3$)(P*i*Pr_3)$_2$] (**7′**). It shows a correlation at δ(^{15}N) –72 with the signal for the metal hydride at δ(^1H) –21.88.[22]

There is no apparent nitrogen coupling on the signal for the metal hydride in the ^{1}H NMR spectrum. This suggests that the ammine ligand and the hydrido ligand are not arranged in a *trans* position at the iridium center.[23] However, the signal at δ 8.36 in the ^{1}H NMR spectrum exhibits an additional coupling to the ^{15}N nucleus of 2.9 Hz. We propose a configuration with the ammine and vinyl ligand in a mutual *trans* arrangement in **7**, although we cannot exclude entirely an isomer with the hydride an the vinyl group in a mutual *trans* position.

Compound **7** transformed completely into the isomers **8a** and **8b** within 8 hours. All NMR spectra reveal two sets of signals, but we were not able to assign them to the according configurations in **8a** or **8b**. The inequivalent phosphorus atoms in both isomers are revealed in the ^{31}P NMR spectrum with phosphorus–phosphorus coupling constants of 336 Hz. The size of the coupling constant is typical for a *trans* arrangement of the two phosphorus containing moieties.[13] Selective decoupling experiments of the alkyl protons give in the ^{31}P NMR for all phosphorus nuclei in **8a** and **8b** a hydrogen coupling of 14 Hz to the corresponding metal bound proton. The ^{1}H NMR spectrum shows signals at δ –21.21 and δ –21.50 for the hydrido ligands at iridium. The spectrum of the ^{15}N labeled isotopologues [Ir(4-C_5NF_4)(H)($^{15}NH_3$){κ^2-(*P,C*)-$CH_2CH(CH_3)PiPr_2$}(P*i*Pr$_3$)] (**8a′** and **8b′**) exhibit no additional ^{15}N coupling which again suggests a *cis* arrangement for the hydride and ammine ligands in both isomers.[23] The presence of the ammine ligands is confirmed by cross-peaks at δ(^{15}N) –75 and δ(^{15}N) –68 in the ^{1}H–^{15}N NMR correlation spectrum.[22]

Treatment of solution of **8a**/**8b** in benzene with dihydrogen gave the dihydrido complex **1** (Scheme 2). However, within two days colourless crystals precipitated from a solution of **8a**/**8b** in benzene. X-Ray crystallographic studies revealed that the precipitate consisted of the N–H activation product [Ir(4-C_5NF_4)(H)(μ-NH_2)(NH_3)(P*i*Pr$_3$)]$_2$ (**9**) (Scheme 3). The latter is insoluble in all common organic solvents. Selected bond lengths and angles of the structure of the binuclear complex **9** are depicted in Fig. 5 and Table 5. The molecule is located on an inversion centre. The bond distances from iridium to nitrogen compare well with the separations found in [Ir(H)(μ-NH_2)(NH_3)(PEt_3)$_2$]$_2$(Cl)$_2$.[12] ^{31}P NMR spectra of the reaction solution showed the formation of free phosphine. Addition of phosphine to a solution of **8a** and **8b** does not inhibit the generation of **9**.

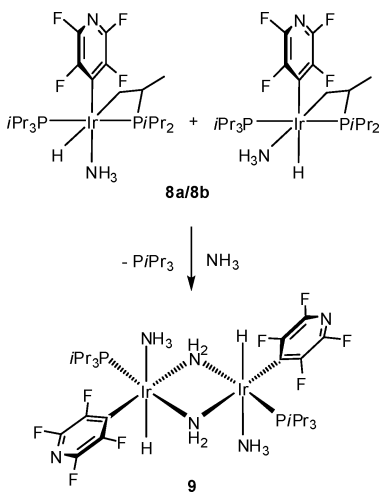

Scheme 3 Oxidative addition of ammonia.

Table 5 Selected bond lengths (Å) and angles (°) in [Ir(4-C_5NF_4)(H)(μ-NH_2)(NH_3)(P*i*Pr$_3$)]$_2$ (**9**) with estimated standard deviations in parentheses

Ir(1)–C(10)	2.036(2)	C(10)–C(11)	1.408(3)
Ir(1)–N(1)	2.1261(18)	C(11)–C(12)	1.368(3)
Ir(1)–N(1)#	2.1243(18)	C(13)–C(14)	1.369(3)
Ir(1)–N(2)	2.239(2)	C(11)–F(1)	1.366(3)
Ir(1)–P(1)	2.2735(6)	C(12)–F(2)	1.354(3)
N(3)–C(13)	1.316(3)	C(13)–F(3)	1.357(3)
N(3)–C(12)	1.317(3)	C(14)–F(4)	1.366(3)
C(10)–C(14)	1.400(3)		
C(10)–Ir(1)–N(1)#	89.40(8)	N(1)#–Ir(1)–P(1)	170.20(5)
C(10)–Ir(1)–N(1)	167.80(8)	Ir(1)#–N(1)–Ir(1)	101.60(8)
C(10)–Ir(1)–N(2)	94.29(8)	N(2)–Ir(1)–P(1)	105.44(5)
C(10)–Ir(1)–P(1)	97.18(6)	C(12)–N(3)–C(13)	113.7(2)
N(1)–Ir(1)–P(1)	94.97(5)	C(11)–C(10)–C(14)	109.4(2)
N(1)–Ir(1)–N(2)	83.51(7)	C(10)–C(11)–C(12)	123.3(2)
Ir(1)–C(10)–C(14)	126.56(17)	C(11)–C(12)–N(3)	125.0(2)
Ir(1)–C(10)–C(11)	123.58(17)	N(3)–C(13)–C(14)	124.9(2)
N(1)#–Ir(1)–N(1)	78.40(8)	C(10)–C(14)–C(13)	123.7(2)
N(1)#–Ir(1)–N(2)	81.18(7)		

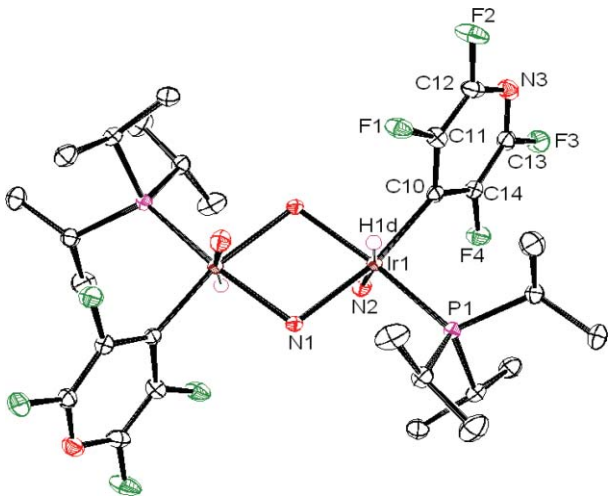

Fig. 5 An ORTEP diagram of **9**; ellipsoids are drawn at the 50% probability level; hydrogen atoms and a benzene solvent molecule have been omitted for clarity, except for metal bound hydrogen.

Discussion

The syntheses of the iridium(III) ammine complexes *cis-trans*-[Ir(4-C_5NF_4)(H)$_2$(NH_3)(P*i*Pr$_3$)$_2$] (**3**), *cis*-[Ir(4-C_5NF_4)(H){(*E*)-(MeO_2C)*C*=CH(CO_2Me)}(NH_3)$_2$(P*i*Pr$_3$)] (**5**) and [Ir(4-C_5NF_4)-(H){κ^2-(*C,O*)-(*Z*)-(MeO_2C)*C*=CH(*CO*OMe)}(NH_3)(P*i*Pr$_3$)] (**6**) are shown in Scheme 1. We did not observe any reactivity of the hydrides or the ammine ligand at one of the metal centers neither upon heating nor under photolytic conditions. Thus a reductive elimination of dihydrogen or of a carbon–hydrogen to give an iridium(I) complex which could be capable for an N–H oxidative addition did not occur. We also have no indication for a C–N coupling reaction at **5** or **6**. Note that it has been reported before that a reaction of $MeO_2CC{\equiv}CCO_2Me$ with ammonia leads to the hydroamination product, even without the presence of a metal centre.[24]

The ethylene complex *trans*-[Ir(4-C_5NF_4)(C_2H_4)(P*i*Pr$_3$)$_2$] (**2**) reacts with ammonia to give *trans*-[Ir(4-C_5NF_4)(H)(C_2H_3)(NH_3)-(P*i*Pr$_3$)$_2$] (**7**), [Ir(4-C_5NF_4)(H)(NH_3){κ^2-(*P,C*)-*C*H_2CH(CH_3)-P*i*Pr$_2$}(P*i*Pr$_3$)] (**8a/8b**) and subsequently [Ir(4-C_5NF_4)(H)(μ-NH_2)(NH_3)(P*i*Pr$_3$)]$_2$ (**9**). At first the oxidative addition of ethylene has been observed to give **7**, but after loss of the olefin ligand cyclometallation of a phosphine ligand occurs. The cyclometallation products **8a/8b** finally transformed into the dinuclear ammine compound **9**. Initial intermediates for the activation steps are presumably either an iridium(I) ammine complex *trans*-[Ir(4-C_5NF_4)(NH_3)(P*i*Pr$_3$)$_2$] (**A**) or the 14-electron species [Ir(4-C_5NF_4)(P*i*Pr$_3$)$_2$] (**B**), one of which reacts in the presence of NH_3 further by oxidative addition of either a C–H bond in the phosphine or a N–H bond in ammonia (Schemes 2–4).

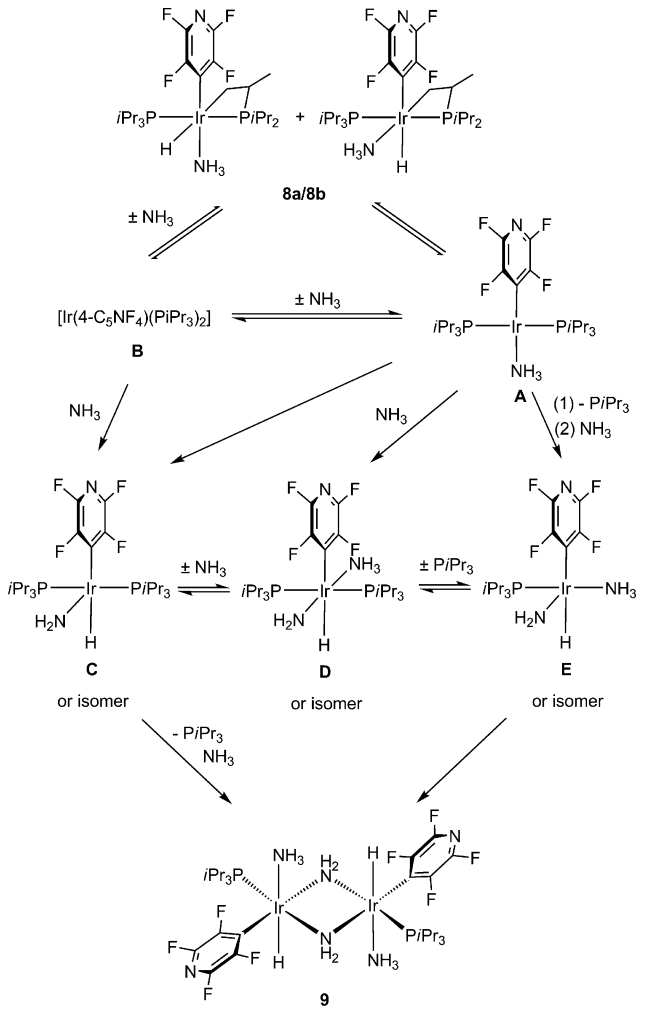

Scheme 4 Proposed mechanism for the formation of **8a/8b** and **9**.

We propose that after C–H reductive elimination in **8a/8b** the ammonia activation occurs at *trans*-[Ir(4-C_5NF_4)(NH_3)-(P*i*Pr$_3$)$_2$] (**A**) or [Ir(4-C_5NF_4)(P*i*Pr$_3$)$_2$] (**B**) to yield *trans*-[Ir(H)(4-C_5NF_4)(NH_2)(P*i*Pr$_3$)$_2$] (**C**), *trans*-[Ir(H)(4-C_5NF_4)(NH_2)(NH_3)-(P*i*Pr$_3$)$_2$] (**D**) or [Ir(H)(4-C_5NF_4)(NH_2)(NH_3)(P*i*Pr$_3$)] (**E**) (Scheme 4) by oxidative addition. The reaction pathways starting from **A** involve oxidative addition of the ammine ligand to give **C**, ammonia coordination followed by N–H activation to yield **D**, and phosphine loss followed by N–H cleavage and ammonia coordination to give **E**. We also can't exclude a direct addition of ammonia at the iridium-carbon bond in **8a** or **8b** or even at cyclometallated derivatives of **B** to give **C**, but the insolubility of **9** does not permit any experiments with ND_3 to elucidate that issue. Phosphine loss at **C** or **D** or dimerisation of **E** gives the binuclear compound **9**, which is very stable because of the bridging amido ligands. We were not able to detect any of the suggested intermediates **A**–**E**; possibly because at **8a/8b** the C–H bond formation might be the rate determining step and also because the generation of **9** is irreversible due to the insolubility of **9**. Free phosphine in the reaction solution does not inhibit the generation of **9**.

The generation of **C** resembles the oxidative addition of ammonia at [Ir{κ^3-(*C,P,P*)-*C*H($CH_2CH_2PtBu_2$)$_2$}(C_2H_4)] to yield [Ir{κ^3-(*C,P,P*)-*C*H($CH_2CH_2PtBu_2$)$_2$}](H)(NH_2)] which has been reported by Zhao, Goldman and Hartwig.[15] In this case the ammonia activation occurs *via* a dissociative pathway by ethylene dissociation to give an intermediate 14-electron species at which the N–H oxidative addition takes place.

N–H oxidative addition can compete with C–H bond cleavage. Schulz and Milstein showed that at *trans*-[Ir(Cl)(C_2H_4)(PEt_3)$_2$] N–H activation of ammonia occurs to give the cationic complex [Ir(H)(μ-NH_2)(NH_3)(PEt_3)$_2$]$_2$(Cl_2), whereas *trans*-[Ir(Cl)(C_2H_4)(P*i*Pr$_3$)$_2$] undergoes, even in the presence of ammonia, C–H activation of ethylene to yield an hydrido vinyl complex.[13] At 353 K a cyclometallation has been observed to give [Ir(Cl)(H){κ^2-(*P,C*)-*i*Pr$_2$*P*CH(Me)*C*H_2}(NH_3)(P*i*Pr$_3$)]. We demonstrated now that C–H activation products such as **7**, **8a** or **8b** can be formed at room temperature and that the C–H activation is reversible to provide an iridium(I) compound as precursor fo a N–H oxidative addition product.

Apparently at {Ir(Cl)(PEt_3)$_2$} a binuclear dicationic complex is formed whereas at {Ir(4-C_5NF_4)(P*i*Pr$_3$)$_2$} the neutral, but also binuclear, species **9** is generated.[2,12] The pincer ligand allows the isolation of the mononuclear compound [Ir(H)(NH_2){κ^3-(*C,P,P*)-*C*H($CH_2CH_2PtBu_2$)$_2$}.[15] It is interesting that at the [Ir{κ^3-(*C,P,P*)-C_6H_3($CH_2CH_2PtBu_2$)$_2$} fragment, which exhibits an aromatic pincer ligand, no oxidative addition of ammonia occurs.[2,21] This has been explained by the better σ–donor capability of the alkyl pincer ligand.[15] However, it appears that the aromatic tetrafluoropyridyl ligand and a chloro ligand also permit N–H activation. Thus the electronic requirements to induce the N–H activation step remain unclear.

Conclusions

We presented N–H and C–H activation reactions at {Ir(4-C_5NF_4)(P*i*Pr$_3$)$_2$} in the presence of ammonia. The C–H activation reactions are reversible and therefore provide access to an N–H oxidative addition pathway of ammonia. The activation of ammonia leads to a dinuclear iridium(III) amido complex **9**.

Experimental

[D_6]Benzene and [D_8]THF were dried by stirring over Na/K and then distilled. Complexes *cis-trans*-[Ir(4-C_5NF_4)(H)$_2$(P*i*Pr$_3$)$_2$] (**1**) and *trans*-[Ir(4-C_5NF_4)(C_2H_4)(P*i*Pr$_3$)$_2$] (**2**) were prepared according to the literature.[16]

The NMR spectra were recorded on a Bruker DPX 300 or Bruker AV 400 spectrometer at 300 K. The ^{1}H NMR chemical shifts were referenced to residual C_6D_5H at δ = 7.15 or [D_7]THF at δ = 1.8 ppm. The ^{19}F NMR spectra were referenced to external C_6F_6 at δ = –162.9 ppm. The ^{31}P{^{1}H} NMR spectra were referenced externally to H_3PO_4 at δ 0.0 ppm. ^{15}N NMR chemical shifts were referenced externellay to 5 M $^{15}NH_4Cl$ in 2 M HCl. Infrared spectra were recorded on a Bruker Vector 22 spectrometer which was equipped with an ATR unit (ZnSe or diamond). Irradiation experiments were carried out with a L.O.T. Xenon lamp (150 W).

Formation of *cis-trans*-[Ir(4-C_5NF_4)(H)$_2$(NH_3)(P*i*Pr$_3$)$_2$] (3)

A slow stream of NH_3 was passed for 1 min through an orange solution of **1** (90 mg, 0.14 mmol) in 10 mL *n*-hexane. The solution turned colourless. The volatiles were removed *in vacuo* to give a colourless solid. Yield 71 mg (78%). Complex **3′** was prepared in a similar manner on using $^{15}NH_3$. Analytical data for **3**: (Found: C, 40.68; H, 6.95; N, 3.40. $C_{23}H_{47}F_4IrN_2P_2$ requires C, 40.52; H, 6.95; N 4.11); $\tilde{\nu}$ (ATR, ZnSe)/cm^{-1} 3407 (NH), 2243, 2037 (IrH); ^{1}H NMR (500 MHz, C_6D_6): δ 1.98–1.71 (m, br, 9 H, C*H*(CH$_3$)$_2$, NH$_3$), 0.91 (s, br, 36 H, CH(C*H*$_3$)$_2$), –14.72 (s, br, 1H, IrH), –24.02 (s, br, 1 H, IrH). ^{19}F NMR (470.4 MHz, C_6D_6): δ –98.6 (m, 1 F), –99.0 (m, 1 F), –104.7 (m, 1 F), –104.8 (m, 1 F). ^{31}P{^{1}H} NMR (202.4 MHz, C_6D_6): δ 30.6 (s).^{1}H,^{15}N HMBC NMR of **3′** (40.5 MHz, C_6D_6): δ(^{15}N) –88.

Formation of *trans*-[Ir(4-C_5NF_4)(H){(*E*)-(MeO$_2$C)*C*=CH(CO$_2$Me)}(P*i*Pr$_3$)$_2$] (4)

MeO$_2$CC≡CCO$_2$Me (33 mg, 0.24 mmol) was added to a solution of **1** (105 mg, 0.16 mmol) in 2 mL toluene. The solution turned red within two hours. After 16 h the volatiles were removed *in vacuo* to give an orange powder, which was extracted with 5 mL *n*–hexane. The extract was stored at –30 °C to obtain **4** as orange crystals. Yield 102 mg (78%). (Found: C, 43.00; H, 6.23; N, 1.55. $C_{29}H_{50}F_4IrNO_4P_2$ requires C, 43.17; H, 6.25; N 1.74); $\tilde{\nu}$ (ATR, diamond)/cm^{-1} 2338 (IrH), 1711 (C=O); ^{1}H NMR (300 MHz, C_6D_6): δ 6.48 (s, 1 H, =CH), 3.48 (s, 3 H, OMe), 3.47 (s, 3 H, OMe), 2.13 (m, 6 H, C*H*(CH$_3$)$_2$), 0.93 (m, 36 H, CH(C*H*$_3$)$_2$), –35.10 (td, J_{HP} = 13.8 Hz, J_{HF} = 4.0 Hz, 1 H, IrH); ^{19}F NMR (282.4 MHz, C_6D_6): δ–99.4 (m, 1 F), –101.6 (m, 1 F), –113.8 (m, 1 F), –117.2 (m, 1 F); ^{31}P{^{1}H} NMR (121.5 MHz, C_6D_6): δ 17.4 (s); ^{13}C NMR (100.6 MHz, C_6D_6): δ 179.5 (s,C=O), 169.0 (s, C=O), 150.6 (s, Ir*C*=C), 133.8 (s, IrC=*C*), 51.8 (s, OCH$_3$), 51.6 (s, OCH$_3$), 26.0 (t, J_{PC} = 13 Hz, *C*HCH$_3$), 19.4 (s, CH*C*H$_3$), 18.8 (s, CH*C*H$_3$), the signals for the fluorinated pyridine ligand were not found.

Formation of *cis*-[Ir(4-C_5NF_4)(H){(*E*)-(MeO$_2$C)*C*=CH(CO$_2$Me)}(NH_3)$_2$(P*i*Pr$_3$)] (5)

A slow stream of NH_3 was passed for 1 min through a solution of **4** (115 mg, 0.19 mmol) in 2 mL benzene. A yellow precipitate formed which consisted of **5**. Yield 94 mg (72%). Complex **5′** was prepared in a similar manner on using $^{15}NH_3$. Analytical data for **5**: (Found: C, 35.81; H, 5.08; N, 5.87. $C_{20}H_{35}F_4IrN_3O_4P$ requires C, 35.29; H, 5.18; N 6.17); $\tilde{\nu}$ (ATR, diamond)/cm^{-1} 3340 (NH), 2239 (IrH), 1740 (C=O), 1690 (C=O); ^{1}H NMR (300 MHz, C_6D_6): δ 6.27 (s, 1 H, =CH), 3.81 (s, 3 H, OMe), 3.67 (s, 3 H, OMe), 3.05 (s, br, for **5′** dd, J_{HP} = 3.6 Hz, J_{HN} = 70.1 Hz, 3 H, NH$_3$), 3.00 (s, br, for **5′** d, J_{HN} = 68.1 Hz, 3 H, NH$_3$), 2.13 (m, 3 H, C*H*(CH$_3$)$_2$), 1.36 (dd, J_{HP} = 7.3 Hz, J_{HH} = 6.3 Hz, 9 H, CH(C*H*$_3$)$_2$), 1.19 (dd, J_{HP} = 7.2 Hz, J_{HH} = 5.7 Hz, 9 H, CH(C*H*$_3$)$_2$), –22.08 (dd, J_{HP} = 23.5 Hz, J_{HF} = 11.5 Hz, for **5′** ddd, additional coupling J_{HN} = 5.6 Hz, 1 H, IrH); ^{19}F NMR (282.4 MHz, [D_8]THF): δ –101.4 (m, 1 F), –102.6 (m, 1 F), –113.4 (m, 1 F), –123.8 (m, 1 F); ^{31}P{^{1}H} NMR (121.5 MHz, [D_8]THF): δ 13.9 (s). ^{31}P{^{1}H} NMR of **5′** (121.5 MHz, [D_8]THF): δ 13.69 (dd, J_{PN} = 46.7 Hz). ^{1}H,^{15}N HMBC NMR of **5′** (40.5 MHz, [D_8]THF): δ(^{15}N) –62; ^{13}C NMR (100.6 MHz, C_6D_6): δ 182.2 (s,C=O), 165.8 (s, C=O), 150.3 (s, Ir*C*=C), 125.9 (s, IrC=*C*), 50.9 (s, OCH$_3$), 50.7 (s, OCH$_3$), 25.7 (t, J_{PC} = 14 Hz, *C*HCH$_3$), 19.6 (s, CH*C*H$_3$), 19.4 (s, CH*C*H$_3$), the signals for the fluorinated pyridine ligand were not found.

Formation of [Ir(4-C_5NF_4)(H){κ^2-(*C*,*O*)-(*Z*)-(MeO$_2$C)*C*=CH(C*O*OMe)}(NH_3)(P*i*Pr$_3$)] (6)

A solution of **5** (33 mg, 0.05 mmol) in 0.5 mL C_6H_6 was transferred into a quartz NMR tube. The reaction mixture was irradiated for 14 h at room temperature. Yellow crystals formed at room temperature which consisted of **6**. Yield 31 mg (98%). Complex **6′** was prepared in a similar manner on using **5′** as starting compound. Analytical data for **6**: (Found: C, 39.44; H, 5.44; N, 4.62. $C_{20}H_{32}F_4IrN_2O_4P \cdot \frac{1}{2}\,C_6H_6$ requires C, 39.31; H, 5.02; N 3.99); $\tilde{\nu}$ (ATR), diamond/cm^{-1} 3340 (NH), 2280 (IrH), 1734 (C=O), 1705 (C=O); ^{1}H NMR (300 MHz, [D_8]THF): δ 6.98 (s, 1 H, =CH), 3.91 (s, 3 H, OMe), 3.66 (s, 3 H, OMe), 2.66 (s, d in the spectrum of **6′**, J_{HN} ≈ 70 Hz, NH$_3$), 2.16 (m, 3 H, C*H*(CH$_3$)$_2$), 1.18 (dd, J_{HP} = 7.2 Hz, J_{HH} = 6.3 Hz, 9 H, CH(C*H*$_3$)$_2$), 0.98 (dd, J_{HP} = 7.3 Hz, J_{HH} = 5.9 Hz, 9 H, CH(C*H*$_3$)$_2$), –28.55 (dd, J_{HP} = 21.9 Hz, J_{HF} = 7.5 Hz); ^{19}F NMR (282.4 MHz, C_6D_6): δ –99.3 (m, 1 F), –100.2 (m, 1 F), –115.6 (m, 1 F), –119.6 (m, 1 F); ^{31}P{^{1}H} NMR (121.5 MHz, C_6D_6: δ 17.3 (s). ^{1}H,^{15}N HMBC NMR of **6′** (40.5 MHz, [D_8]THF): δ(^{15}N) –55.

Treatment of *trans*-[Ir(4-C_5NF_4)(C_2H_4)(P*i*Pr$_3$)$_2$] (2) with ammonia

A slow stream of NH_3 was passed for 30 s through a red solution of **2** (40 mg, 0.06 mmol) in 2 mL C_6D_6. The NMR spectroscopic data of the solution reveal the initial formation of **7**, **8a** and **8b** (ratio **2** : **7** : **8a** : **8b** after 3 h: 13 : 17 : 27 : 43). After 8 h only **8a** and **8b** could be detected. The ^{1}H NMR specrum showed the formation of free ethylene. After 2d colourless crystals of **9** precipitated which were identified by X-ray crystallography. The complexes **7′**, **8a′** and **8b′** were prepared in a similar manner on using $^{15}NH_3$. Analytical data for **7**: ^{1}H NMR (500 MHz, C_6D_6): δ 8.36 (m, dd, $J_{HH,trans}$ = 19.6 Hz, $J_{HH,cis}$ = 12.6 Hz, for **7′** additional doublet coupling of J_{HN} = 2.9 Hz, 1 H, C*H*= CH$_2$), 6.03 (d, $J_{HH,cis}$ = 12.5 Hz, 1 H, CH= C*H*H), 5.02 (dd, $J_{HH,trans}$ = 20.0 Hz, J_{HH} = 3.0 Hz, 1 H, CH= C*H*H), 2.51 (s, br, NH$_3$), 2.11 (m, J_{HH} = 7.2 Hz, 6 H, C*H*(CH$_3$)$_2$), 0.87 (dvt, J_{HH} = 7.2 Hz, N = 7.0 Hz, 36 H, CH(C*H*$_3$)$_2$), –21.88 (dt, J_{HP} = 17.4 Hz, J_{HF} = 9.3 Hz, 1 H, IrH); the coupling constants were confirmed by ^{19}F and ^{31}P decoupling; ^{19}F NMR (282.4 MHz, C_6D_6): δ –101.1 (m, 1 F), –103.1 (m, 1 F), –109.8 (m, 1 F), –123.9 (m, 1 F); ^{31}P{^{1}H} NMR (202.4 MHz, C_6D_6): δ = 1.8 (s). ^{1}H,^{15}N HMBC NMR of **7′** (40.5 MHz, C_6D_6): δ(^{15}N) –72. Analytical data for **8a**: ^{1}H–NMR (500 MHz, C_6D_6): δ 2.13 (s, d in the spectrum of **8a′**, J_{HN} ≈ 75 Hz, NH$_3$), –21.21 (m, d in the ^{1}H{^{31}P} NMR,

Table 6 Crystallographic data

Compound	**3**	**4**[a]	**5**	**6**	**9**
Crystal dimensions/mm^3	0.20 × 0.16 × 0.08	0.24 × 0.12 × 0.08	0.20 × 0.15 × 0.12	0.36 × 0.34 × 0.28	0.23 × 0.12 × 0.08
Empirical formula	$C_{23}H_{47}F_4IrN_2P_2$	$C_{29}H_{50}F_4IrNO_4P_2$	$C_{26}H_{41}F_4IrN_3O_4P$	$C_{23}H_{35}F_4IrN_2O_4P$	$C_{34}H_{60}F_8Ir_2N_6P_2$
Formula weight	681.77	806.84	758.79	702.70	1151.22
Crystal system	Triclinic	Orthorhombic	Monoclinic	Monoclinic	Monoclinic
Space group	$P\bar{1}$	$P2_12_12_1$	$P2_1/n$	$P2_1/n$	$P2_1/c$
a/Å	8.7052(14)	10.7834 (16)	10.7140(3)	14.7892(4)	13.6890 (2)
b/Å	10.2909(19)	14.3514 (16)	13.1461(3)	10.4836(2)	9.9290 (2)
c/Å	16.232(3)	21.382(3)	21.3446(5)	17.1372(5)	15.0110 (2)
α/°	75.886(15)	—	—	—	—
β/°	86.624(14)	—	93.574(2)	98.780(7)	92.8640(10)
γ/°	73.932(13)	—	—	—	—
V/Å^3	1355.1(4)	3309.0(7)	3000.48(13)	2625.89(12)	2037.72 (6)
Z	2	4	4	4	2
Density (calcd.)/Mg m^{-3}	1.671	1.620	1.680	1.777	1.876
μ(Mo Kα)/mm^{-1}	5.086	4.187	4.563	5.205	6.672
θ range/°	2.59 to 27.50	2.36 to 25.50	3.34 to 29.00	2.41 to 28.75	2.91 to 27.50
Reflections collected	22666	32822	49585	47604	47134
Independent reflections	6215	6150	7955	6817	4653
R_{int}	0.0576	0.0385	0.1414	0.0952	0.038
Goodness-of-fit on F^2	1.007	0.915	0.836	0.953	1.049
R_1, wR_2 on all data	0.0222, 0.0511	0.0215, 0.0276	0.1059, 0.0762	0.0255, 0.0415	0.0186, 0.0340
R_1, wR_2 [$I_o > 2\sigma(I_o)$]	0.0201, 0.0504	0.0158, 0.0272	0.0436, 0.0653	0.0187, 0.0403	0.0159, 0.0332
Reflect. with $I_o > 2\sigma(I_o)$]	5845	5505	4591	5946	4306
Max diff peak, hole/e Å^{-3}	2.545 and –1.920	0.599 and –0.472	2.812 and –2.805	1.545 and –0.954	0.956 and –0.575

[a] Flack parameter: –0.014(3).

J_{HF} = 9.5 Hz, vt in the $^1H\{^{19}F\}$ NMR, J_{HP} = 16.3 Hz, IrH). The resonances for the *i*Pr groups are obscured by signals of **8b**. ^{19}F NMR (564.6 MHz, C_6D_6): δ –100.9 (m, 1 F), –102.0 (m, 2 F), –103.5 (m, 1 F). $^{31}P\{^1H$-selective$\}$ NMR (162.0 MHz, C_6D_6): δ 13.0 (dd, J_{PP} = 336 Hz, J_{PH} = 16 Hz), –36.5 (dd, J_{PP} = 336 Hz, J_{PH} = 14 Hz).$^1H,^{15}N$ HMBC NMR of **8a′** (40.5 MHz, C_6D_6): $\delta(^{15}N)$ –75. Analytical data for **8b**: ^1H NMR (500 MHz, C_6D_6): δ –21.50 (m, d in the $^1H\{^{31}P\}$ NMR, J_{HF} = 6.5 Hz, vt in the $^1H\{^{19}F\}$ NMR, J_{HP} = 15.3 Hz, IrH). The resonances for the *i*Pr groups are obscured by signals of **8a**. ^{19}F NMR (564.6 MHz, C_6D_6): δ –100.9 (m, 1 F), –104.7 (m, 1 F), –124.8 (m, 1 F), –125.5 (m, 1 F). $^{31}P\{^1H$-selective$\}$ NMR (162.0 MHz, C_6D_6): δ 10.9 (dd, J_{PP} = 336 Hz, J_{PH} = 14 Hz), –28.1 (dd, J_{PP} = 336 Hz, J_{PH} = 14 Hz). $^1H,^{15}N$ HMBC NMR of **8b′** (40.5 MHz, C_6D_6): $\delta(^{15}N)$ –68. Analytical data for **9**: (Found: C, 36.02; H, 5.57; N, 7.33. $C_{28}H_{54}F_8Ir_2N_6P_2C_6H_6$ requires C, 35.47; H, 5.25; N 7.30); $\tilde{\nu}$ (ATR, diamond)/cm^{-1} 3391, 3351 (NH), 2238 (IrH).

Structure determinations for the complexes 3, 4, 5, 6 and 9†

Colourless crystals of **3** and **9** and yellow crystals of **4–6** were obtained from a solution in hexane at 243 °C. The diffraction data for complex **9** were collected on a Nonius Kappa CCD diffractometer at 100 K. Diffraction data for **3**, **5** and **6** were collected on a STOE IPDS 2T diffractometer at 100 K, whereas the data for **4** were collected on a STOE IPDS diffractometer at 170 K. Crystallographic data are depicted in Table 6. The structures were solved by direct methods (SHELXTL PLUS or SIR 97) and refined with the full matrix least square methods on F^2 (SHELX-97).[25–27] Hydrogen atoms were placed at calculated positions and refined using a riding model. For complex **3**, **4**, **6** and **9** the metal bound hydrogens were located in the difference fourier and refined isotropically. The hydrogen atom bound at Ir in **5** was not located.

Acknowledgements

We thank the "Fonds der Chemischen Industrie" for financial support. The authors also acknowledge support from the Cluster of Excellence "Unifying Concepts in Catalysis" funded by the Deutsche Forschungsgemeinschaft. We are grateful to S. Hinze for experimental assistance. We also thank P. Neubauer the X-ray crystallography (**3–6**) as well as Dr B. Ziemer, and A. Penner for helpful discussions concerning the crystal structure analyses.

References

1 R. Severin and S. Doye, *Chem. Soc. Rev.*, 2007, **36**, 1407–1420; K. C. Hultzsch, *Adv. Synth. Catal.*, 2005, **347**, 367–391; M. Beller, J. Seayad, A. Tillack and H. Jiao, *Angew. Chem.*, 2004, **116**, 3448–3479; M. Beller, J. Seayad, A. Tillack and H. Jiao, *Angew. Chem. Int. Ed.*, 2004, **43**, 3368–3398; F. Alonso, I. P. Beletskaya and M. Yus, *Chem. Rev.*, 2004, **104**, 3079–3160; P. W. Roesky and T. E. Müller, *Angew. Chem.*, 2003, **115**, 2812–2814; P. W. Roesky and T. E. Müller, *Angew. Chem. Int. Ed.*, 2003, **42**, 2708–2710; J. Seayad, A. Tillack, G. C. Hartung and M. Beller, *Adv. Synth. Catal.*, 2002, **344**, 795–813; I. Bytschkov and S. Doye, *Eur. J. Org. Chem.*, 2003, 935–946; F. Pohlki and S. Doye, *Chem. Soc. Rev.*, 2003, 104–114; S. Doye, *Synlett*, 2004, 1653–1672.

2 T. Braun, *Angew. Chem.*, 2005, **117**, 5138–5140; T. Braun, *Angew. Chem Int. Ed.*, 2005, **44**, 5012–5014.

3 D. S. Surry and S. L. Buchwald, *J. Am. Chem. Soc.*, 2007, **129**, 10354–10355; Q. Shen and J. F. Hartwig, *J. Am. Chem. Soc.*, 2006, **128**, 10028–10029; M. C. Willis, *Angew. Chem.*, 2007, **119**, 3470–3472; M. C. Willis, *Angew. Chem., Int. Ed.*, 2007, **46**, 3402–3404; J. Kim and S. Chang, *Chem. Commun.*, 2008, 3052–3054; R. Ntaganda, B. Dhudshia, C. L. B. Macdonald and A. N. Thadani, *Chem. Commun.*, 2008, 6200–6202; N. Xia and M. Taillefer, *Angew. Chem.*, 2009, **121**, 343–345; N. Xia and M. Taillefer, *Angew. Chem. Int. Ed.*, 2009, **48**, 337–339; H. Rao, H. Fu, Y. Jiang and Y. Zhao, *Angew. Chem.*, 2009, **121**, 1134–1136; H. Rao, H. Fu, Y. Jiang and Y. Zhao, *Angew. Chem. Int. Ed.*, 2009, **48**, 1114–1116.

4 T. Gross, A. M. Seayad, M. Ahmad and M. Beller, *Org. Lett.*, 2002, **4**, 2055–2058.

5 C. Gunanathan and D. Milstein, *Angew. Chem.*, 2008, **120**, 8789–8792; C. Gunanathan and D. Milstein, *Angew. Chem. Int. Ed*, 2008, **47**, 8661–8664.

6 V. Lavallo, G. D. Frey, B. Donnadieu, M. Soleilhavoup and G. Bertrand, *Angew. Chem.*, 2008, **120**, 5302–5306; V. Lavallo, G. D. Frey, B. Donnadieu, M. Soleilhavoup and G. Bertrand, *Angew. Chem. Int. Ed.*, 2008, **47**, 5224–5228.

7 E. N. Nishina and Y. Yamamoto, *Angew. Chem.*, 2006, **118**, 3392–3395; E. N. Nishina and Y. Yamamoto, *Angew. Chem. Int. Ed.*, 2006, **45**, 3314–3317.

8 E. Mizushima, T. Hayashi and M. Tanaka, *Org. Lett.*, 2003, **5**, 3349–3352.

9 M. M. B. Holl, P. T. Wolczanski and G. D. Van Duyne, *J. Am. Chem. Soc.*, 1990, **112**, 7989–7994; J. E. Bercaw, D. L. Davies and P. T. Wolczanski, *Organometallics*, 1986, **5**, 443–450; H. W. Roesky, Y. Bai and M. Noltemeyer, *Angew. Chem.*, 1989, **101**, 788–789; H. W. Roesky, Y. Bai and M. Noltemeyer, *Angew. Chem. Int. Ed.*, 1989, **28**, 754–755; J. N. Armor, *Inorg. Chem.*, 1978, **17**, 203–213; G. L. Hillhouse and J. E. Bercaw, *J. Am. Chem. Soc.*, 1984, **106**, 5472–5478; D. Connor, K. N. Jayaprakash, T. R. Cundari and T. B. Gunnoe, *Organometallics*, 2004, **23**, 2724–2733; D. M. Roundhill, *Chem. Rev.*, 1992, **92**, 1–27; M. V. Ovchinnikov, E. LeBlanc, I. A. Guzei and R. J. Anglici, *J. Am. Chem. Soc.*, 2001, **123**, 11494–11495; A.-M. Fuller, W. Clegg, R. W. Harrington, D. L. Hughes and S. J. Lancaster, *Chem. Commun.*, 2008, 5778–5778; P. Avenier, A. Lesage, M. Taoufik, A. Baudouin, A. De Mallmann, S. Fiddy, M. Vautier, L. Veyre, J.-M. Basset, L. Emsley and E. A. Quadrelli, *J. Am. Chem. Soc.*, 2007, **129**, 176–186; J. S. Freundlich, R. R. Schrock and W. M. Davis, *J. Am. Chem. Soc.*, 1996, **118**, 3643–3655; I. Aviv and Z. Gross, *Chem. Commun.*, 2006, 4477–4479; K. Koszinowski, M. Schlangen, D. Schröder and H. Schwarz, *Int. J. Mass. Spectr.*, 2004, **217**, 19–23; K. Koszinowski, D. Schröder and H. Schwarz, *J. Phys. Chem. A*, 2003, **107**, 4999–5006; Y. Nakajima, H. Kameo and H. Suzuki, *Angew. Chem.*, 2006, **118**, 964–966; Y. Nakajima, H. Kameo and H. Suzuki, *Angew. Chem. Int. Ed.*, 2006, **45**, 950–952; T. Zweifel, J.-V. Naubron and H. Grützmacher, *Angew. Chem.*, 2009, **121**, 567–571; T. Zweifel, J.-V. Naubron and H. Grützmacher, *Angew. Chem. Int. Ed.*, 2009, **48**, 559–563; M. Käß, A. Friedrich, M. Drees and S. Schneider, *Angew. Chem.*, 2009, **121**, 922–924; M. Käß, A. Friedrich, M. Drees and S. Schneider, *Angew. Chem. Int. Ed.*, 2009, **48**, 905–907.

10 R. Koelliker and D. Milstein, *J. Am. Chem. Soc.*, 1991, **113**, 8524–8525.

11 G. Süß-Fink, *Z. Naturforsch. B.*, 1980, **35B**, 454–457; E. G. Bryan, B. F. G. Johnson and J. Lewis, *J. Chem. Soc. Dalton Trans.*, 1977, 1328–1330.

12 A. L. Casalnuovo, J. C. Calabrese and D. Milstein, *Inorg. Chem.*, 1987, **26**, 971–973; R. Koelliker and D. Milstein, *Angew. Chem.*, 1991, **103**, 724–726; R. Koelliker and D. Milstein, *Angew. Chem. Int. Ed.*, 1991, **30**, 707–709.

13 M. Schulz and D. Milstein, *Chem. Commun.*, 1993, 318–319.

14 T. E. Hanna, E. Lobkovski and P. J. Chirik, *Eur. J. Inorg. Chem.*, 2007, 2677–2685; C. M. Farfard, D. Adhikari, B. M. Foxman, D. J. Mindiola and O. V. Ozerov, *J. Am. Chem. Soc.*, 2007, **129**, 10318–10319; S. A. Macgregor, *Organometallics*, 2001, **20**, 1860–1874 for an oxidative addition at Sn see; Y. Peng, B. D. Ellis, X. Wang and P. P. Power, *J. Am. Chem. Soc.*, 2008, **130**, 12268–12269; G. D. Frey, V. Lavallo, B. Donnadieu, W. W. Schoeller and G. Bertrand, *Science*, 2007, **316**, 439–441.

15 J. Zhao, A. S. Goldman and J. F. Hartwig, *Science*, 2005, **307**, 1080–1082.

16 M. Ahijado Salomon, T. Braun and I. Krossing, *Dalton Trans.*, 2008, 5197–5206.

17 M. A. García-Monforte, P. J. Alonso, J. Forníes and B. Menjón, *Dalton Trans.*, 2007, 3347–3359; A. Steffen, T. Braun, B. Neumann and H.-G. Stammler, *Angew. Chem.*, 2007, **119**, 8828–8832; A. Steffen, T. Braun, B. Neumann and H.-G. Stammler, *Angew. Chem. Int. Ed.*, 2007, **46**, 8674–8678; M. Ahijado and T. Braun, *Angew. Chem.*, 2008, **120**, 2996–3000; M. Ahijado and T. Braun, *Angew. Chem.*, 2008, **47**, 2954–2958; T. Braun, B. Blöcker, V. Schorlemer, B. Neumann, A. Stammler and H.-G. Stammler, *J. Chem. Soc., Dalton Trans.*, 2002, 2213–2218; D. Noveski, T. Braun, B. Neumann, A. Stammler and H.-G. Stammler, *Dalton Trans.*, 2004, 4106–4119; M. Ahijado, T. Braun, D. Noveski, N. Kocher, B. Neumann, D. Stalke and H.-G. Stammler, *Angew. Chem.*, 2005, **117**, 7107–7111; M. Ahijado, T. Braun, D. Noveski, N. Kocher, B. Neumann, D. Stalke and H.-G. Stammler, *Angew. Chem. Int. Ed.*, 2005, **44**, 6947–6951; T. Braun, J. Izundu and A. Steffen, *Dalton Trans.*, 2006, **43**, 5118–5123; M. Ahijado-Salomom, T. Braun and A. Penner, *Angew. Chem.*, 2008, **120**, 8999–9003; M. Ahijado-Salomom, T. Braun and A. Penner, *Angew. Chem., Int. Ed.*, 2008, **47**, 8967–8871; A. Steffen, M. I. Sladek, T. Braun, B. Neumann and H.-G. Stammler, *Organometallics*, 2005, **23**, 4057–4064; T. Braun, V. Schorlemer, B. Neumann and H.-G. Stammler, *J. Fluorine Chem.*, 2006, **127**, 367–372; M. I. Sladek, T. Braun, B. Neumann and H.-G. Stammler, *New. J. Chem.*, 2003, **27**, 313–318.

18 T. Braun, D. Noveski, M. Ahijado and F. Wehmeier, *Dalton Trans.*, 2007, 3820–3825.

19 T. Dirnberger and H. Werner, *Inorg. Chim. Acta*, 2007, **360**, 1339–1343; H. Werner, T. Dirnberger and M. Schulz, *Angew. Chem.*, 1988, **100**, 993–994; H. Werner, T. Dirnberger and M. Schulz, *Angew. Chem. Int. Ed.*, 1988, **27**, 948–950.

20 M. A. Esteruelas, M. P. García, M. Martín, O. Nürnberg and L. A. Oro, *J. Organomet. Chem.*, 1994, **466**, 249–257.

21 L. Dahlenburg and K. Herbst, *J. Chem. Soc. Dalton Trans.*, 1999, 3935–3939.

22 M. Kanzelberger, X. Zhang, T. J. Emge, A. S. Goldman, J. Zhao, C. Incarvito and J. F. Hartwig, *J. Am. Chem. Soc.*, 2003, **125**, 13644–13645.

23 A. S. Goldman and J. Halpern, *J. Organomet. Chem.*, 1990, **382**, 237–253.

24 R. Huisgen, K. Herbig, A. Siegl and H. Huber, *Chem. Ber.*, 1966, **99**, 2546–2555.

25 *SHELXTL-PLUS, Siemens Analytical X-Ray Instruments Inc.*, Madison, Wisconsin, USA, 1990.

26 G. M. Sheldrick, *Acta Crystallogr., Sect. A*, 2008, **64**, 112.

27 G. Cascarano, A. Altomare, C. Giacovazzo, A. Guagliardi, A. G. G. Moliterni, D. Sigli, M. C. Burla, G. Polidori and M. Camalli, *Acta Crystallogr.*, 1996, **A52**, C79.